Laboratory Investigation (2020) 100:285–296
https://doi.org/10.1038/s41374-019-0341-7

ARTICLE

Vascular endothelial growth factor enhances profibrotic activities through modulation of calcium homeostasis in human atrial fibroblasts

Cheng-Chih Chung[1,2] · Yung-Kuo Lin[1,2] · Yao-Chang Chen[3] · Yu-Hsun Kao[4,5] · Ting-I Lee[6,7] · Yi-Jen Chen[2,4,8]

Received: 20 April 2019 / Revised: 14 September 2019 / Accepted: 16 October 2019 / Published online: 20 November 2019

Abstract

Vascular endothelial growth factor (VEGF), a pivotal activator of angiogenesis and calcium (Ca^{2+}) signaling in endothelial cells, was shown to increase collagen production in atrial fibroblasts. In this study, we evaluated whether VEGF may regulate Ca^{2+} homeostasis in atrial fibroblasts and contribute to its profibrogenesis. Migration, and proliferation analyses, patch-clamp assay, Ca^{2+} fluorescence imaging, and western blotting were performed using VEGF-treated (300 pg/mL or 1000 pg/mL) human atrial fibroblasts with or without coadministration of Ethylene glycol tetra-acetic acid (EGTA, 1 mmol/L), or KN93 (a Ca^{2+}/calmodulin-dependent protein kinase II [CaMKII] inhibitor, 10 μmol/L). VEGF (1000 pg/mL) increased migration, myofibroblast differentiation, pro-collagen type I, pro-collagen type III production, and phosphorylated VEGF receptor 1 expression of fibroblasts. VEGF (1000 pg/mL) increased the nonselective cation current (I_{NSC}) of transient receptor potential (TRP) channels and potassium current of intermediate-conductance Ca^{2+}-activated K^+ ($K_{Ca}3.1$) channels thereby upregulating Ca^{2+} entry. VEGF upregulated phosphorylated ERK expression. An ERK inhibitor (PD98059, 50 μmol/L) attenuated VEGF-activated I_{NSC} of TRP channels. The presence of EGTA attenuated the profibrotic effects of VEGF on pro-collagen type I, pro-collagen type III production, myofibroblast differentiation, and migratory capabilities of fibroblasts. VEGF upregulated the expression of phosphorylated CaMKII in fibroblasts, which was attenuated by EGTA. In addition, KN93 reduced VEGF-increased pro-collagen type I, pro-collagen type III production, myofibroblast differentiation, and the migratory capabilities of fibroblasts. In conclusion, we found that VEGF increases atrial fibroblast activity through CaMKII signaling by enhancing Ca^{2+} entry. Our findings provide benchside evidence leading to a potential novel strategy targeting atrial myopathy and arrhythmofibrosis.

✉ Ting-I Lee
agleems29@gmail.com

✉ Yi-Jen Chen
yjchen@tmu.edu.tw

[1] Division of Cardiology, Department of Internal Medicine, School of Medicine, College of Medicine, Taipei Medical University, Taipei, Taiwan

[2] Division of Cardiovascular Medicine, Department of Internal Medicine, Wan Fang Hospital, Taipei Medical University, Taipei, Taiwan

[3] Department of Biomedical Engineering, National Defense Medical Center, Taipei, Taiwan

[4] Graduate Institute of Clinical Medicine, College of Medicine, Taipei Medical University, Taipei, Taiwan

[5] Department of Medical Education and Research, Wan Fang Hospital, Taipei Medical University, Taipei, Taiwan

[6] Department of General Medicine, School of Medicine, College of Medicine, Taipei Medical University, Taipei, Taiwan

[7] Division of Endocrinology and Metabolism, Department of Internal Medicine, Wan Fang Hospital, Taipei Medical University, Taipei, Taiwan

[8] Cardiovascular Research Center, Wan Fang Hospital, Taipei Medical University, Taipei, Taiwan

Introduction

Vascular endothelial growth factor (VEGF) plays a pivotal role in cardiovascular disease. Tissue or serum levels of VEGF have been described to represent tissue hypoxia or angiogenesis status in patients with atrial fibrillation (AF) [1], acute myocardial infarction [2], and heart failure [3]. VEGF is highly expressed in atrial tissue and intra-atrium serum of patients with atrial arrhythmia [1, 4, 5]. In addition, VEGF in peri-atrial adipose tissue is highly correlated with atrial fibrosis levels in patients with AF [6]. A recent epidemiological study suggested that VEGF is an important risk factor for AF and ischemic stroke [7]. In hypertensive rats, VEGF is greatly coexpressed with myofibroblasts in the pulmonary veins-atrial junction [8]. These findings support the hypothesis that VEGF may play an important role in the pathophysiology of fibrotic atrial myopathy. However, the association between VEGF and fibrogenesis has not been fully elucidated. Previous studies have revealed that VEGF overexpressing mice have higher degrees of ventricular fibrosis than knockout mice [9]. VEGF can increase migratory and collagen production capabilities of human skin fibroblasts [10], and rat ventricular fibroblasts through ERK signaling pathway [11]. VEGF exerts its profibrotic effect by inducing myofibroblast transformation in conjunctival epithelial cells [12]. VEGF can activate higher collagen production in chondrocytes via the P38 signaling pathway [13]. Similarly, our recent study showed that VEGF can significantly increase collagen production in rat left atrial fibroblasts [14]. However, the cellular mechanisms underlying the effects of VEGF on atrial fibroblasts were not fully elucidated.

The calcium (Ca^{2+}) signaling pathway has been demonstrated to be the downstream signaling of multiple profibrotic cytokines [15, 16]. Increasing Ca^{2+} influx augments myofibroblast differentiation [17], and proliferation [18], collagen production [19], and migratory capabilities of fibroblasts [20]. Moreover, VEGF can promote the proliferative capability of endothelial cells by increasing Ca^{2+} influx [21]. Nevertheless, the profibrotic effect of VEGF induced by Ca^{2+} signaling in human atrial fibroblasts is unclear. The purpose of this study was to examine whether VEGF regulates atrial fibrogenesis through modulation of fibroblast activity and Ca^{2+} homeostasis.

Materials and methods

Cell cultures

Human atrial fibroblasts were obtained from Lonza Research Laboratory (Walkersville, MD, USA). Cells were seeded on uncoated culture dishes as monolayers in Dulbecco's modified Eagle's medium (Thermo Fisher Scientific, Loughborough, UK) containing 10% fetal bovine serum (HyClone Laboratories, Logan, UT, USA) and 100 U/mL penicillin–streptomycin (Thermo Fisher Scientific, Loughborough, UK) at 37 °C with 5% CO_2. Cells from passages 4–6 were used in this study to avoid the possible variations in cellular function.

Cell migration assay

Migration of atrial fibroblasts, treated with VEGF-A (300 pg/mL, 1000 pg/mL, Sigma-Aldrich, St. Louis, MO, USA), with or without ethylene glycol tetra-acetic acid (EGTA, 1 mmol/L, Sigma-Aldrich) or a Ca^{2+}/calmodulin-dependent protein kinase II (CaMKII) inhibitor (KN93, 10 µmol/L, Sigma-Aldrich), was analyzed using a wound-healing assay 6 h after a cell monolayer in a six-well plate was scraped using a P200 pipette tip. Each gap length was assessed using SPOT software (SPOT imaging, Sterling Heights, MI, USA) and calculated from the average of 12 regions. The net migration distance after 6 h was subtracted from that at the time of the initial scratch [14].

Cell proliferation assay

Atrial fibroblast proliferation was measured using a commercial MTS kit (Promega, Madison, WI, USA) as previously described [22]. Briefly, atrial fibroblasts were seeded onto a 96-well culture dish at a density of 3000 cells/well. After growing to 50% confluence, the cells were incubated in serum-free medium with VEGF-A (300 pg/mL, 1000 pg/mL) for 24 h. Cell growth was analyzed using the MTS reagent, which was added 4 h before spectrophotometric analysis was performed.

Western blotting

Western blotting was performed as described previously [14]. Atrial fibroblasts treated with VEGF-A (300 pg/mL, 1000 pg/mL), with or without EGTA (1 mmol/L), or KN93 (10 µmol/L) were homogenized and lysed in radioimmunoprecipitation assay buffer containing 50 mmol/L Tris pH 7.4, 150 mmol/L NaCl, 1% Nonidet P P40, 0.5% sodium deoxycholate, 0.1% sodium dodecyl sulfate (SDS) and protease inhibitor cocktails (Sigma-Aldrich). The protein concentration was determined using a Bio-Rad protein assay reagent (Bio-Rad Laboratories, Hercules, CA, USA). Proteins were separated on a 10% SDS-polyacrylamide gel electrophoresis gel under reducing conditions and electrophoretically transferred onto an equilibrated polyvinylidene difluoride membrane (Amersham Biosciences, Buckinghamshire, UK). Blots were probed with primary antibodies against phosphorylated VEGF receptor 1 (pVEGFR1,

1:500, polyclonal, GeneTex Inc., Irvine, CA, USA), total VEGF receptor 1 (tVEGFR1, 1:1000, monoclonal, clone number: Y103, Abcam, Cambridge, UK), α-smooth muscle actin (SMA) (1:1000, monoclonal, clone number: 1A4, Abcam), pro-collagen type IA1(1:500, monoclonal, clone number: 3G3, Santa Cruz Biotechnology, Santa Cruz, CA, USA), pro-collagen type III(1:1000, monoclonal, clone number: FH7A, Abcam), phosphorylated ERK 1/2 (pERK, 1:1000, monoclonal, and clone number: D13.14.4E, Cell Signaling Technology, Beverly, MA, USA), phosphorylated p38 (pp38, 1:1000, Polyclonal, Cell Signaling Technology), phosphorylated CaMKII (1:2000, polyclonal, Abcam), and total CaMKII (1:2000, polyclonal, GeneTex Inc.). The blots were then incubated with secondary antibodies conjugated with horseradish peroxidase. Bound antibodies were detected using an enhanced chemiluminescence detection system (Millipore, Darmstadt, Germany) and analyzed with AlphaEaseFC software (Alpha Innotech, San Leandro, CA, USA). Targeted bands were normalized to the glyceraldehyde 3-phosphate dehydrogenase protein (Sigma-Aldrich) to confirm equal protein loading and then normalized to the value of control cells.

Patch-clamp experiments

A whole-cell patch clamp was used on detached single fibroblast using an Axopatch 1D amplifier (Axon Instruments, Foster City, CA, USA). Borosilicate glass electrodes (o.d., 1.8 mm) with tip resistances of 3–5 MΩ were used. The area under the capacitive current was initiated by a small hyperpolarizing step from a holding potential of −50 mV to a test potential of −55 mV for 80 ms. When measuring nonselective cation currents (I_{NSC}) through transient receptor potential (TRP) channels, we superfused the detached fibroblasts with Tyrode solution containing the following (in mmol/L): NaCl 140, tetraethylammonium chloride 5.4, MgCl 1.0, $CaCl_2$ 2.0, glucose 10, and 4-(2-hydroxyethyl)-1-piperazineethanesulfonic acid (HEPES) 10 with pH 7.4 adjusted with CsOH. The pipette solution contained the following (in mmol/L): $CsCl_2$ 135, $CaCl_2$ 0.1, EGTA 10, magnesium adenosine triphosphate (Mg-ATP) 4.0, $MgCl_2$ 1.0, HEPES 10, sodium guanosine triphosphate 0.3, and Na2-phosphocreatine 6.6 with pH 7.4 adjusted with CsOH. The currents were the differences before and after gadolinium (100 μmol/L; sigma) recorded by a voltage ramps for 3 s, ranging from −110 to +100 mV (0.07 mV/ms, 0.1 Hz) at 37 °C. Nifedipine (5 μmol/L) was used in external solution to block any L-type Ca^{2+} current.

When measuring potassium currents through intermediate-conductance Ca^{2+}-activated K^+ channels ($K_{Ca}3.1$), we superfused the detached fibroblasts with Tyrode solution containing the following (in mmol/L): NaCl 136, KCl 5.4, MgCl 1.0, $CaCl_2$ 1.8, glucose 10, and HEPES 10 with pH 7.4 adjusted with KOH. The pipette solution contained the following (in mmol/L): KCl 20, K-aspartate 120, $MgCl_2$ 1.0, EGTA 5.0, HEPES 10, GTP 0.1, Na2-phosphocreatine 5.0, Mg-ATP 5.0, and free Ca^{2+} 500 nmol/L, with pH 7.2 adjusted with KOH. The currents were measured as the differences before and after TRAM-34 (1 μmol/L, Sigma-Aldrich) recorded through a voltage STEP for 0.3 s, ranging from −100 to +60 mV with holding potential at −70 mV at 22 °C

Intracellular Ca^{2+} imaging

Ca^{2+} imaging was conducted as described previously [23]. Atrial fibroblasts on 3 cm glass bottom chamber slides were loaded with fura-2-acetoxymethyl ester (5 μmol/L, Life Technologies, Carlsbad, CA, USA) and Pluronic F-127 (20% solution in dimethyl sulfoxide; 2.5 μg/mL) in a Ca^{2+}-free solution containing the following (in mmol/L) NaCl 120, KCl 5.4, KH2PO4 1.2, MgSO4 1.2, glucose 10, HEPES 6 and taurine 8 (pH 7.40) for 30 min at 36 °C in a humidified incubator with 5% CO_2. Fura-2 fluorescence images were captured using a Polychrome V monochromator (Till Photonics, Munich, Germany) mounted on an upright Leica DMI 3000B microscope (Leica Microsystems, Buffalo Grove, IL, USA) with dual-excitation wavelengths of 340 and 380 nm, and an emission wavelength of 510 nm. Fura-2 images were analyzed using MetaFluor software version 7.7.6.0 (Molecular Devices, Sunnyvale, CA, USA). The ratio of fluorescence due to excitation at 340 nm (F_{340}) to F_{380} was used as a marker of the relative level of intracellular Ca^{2+}. To measure Ca^{2+} entry, cells were first exposed to the Ca^{2+}-free solution for 8 min. The extracellular Ca^{2+} concentration was then increased to 2 mmol/L to measure Ca^{2+} entry via store-operated channels activated by Ca^{2+}-store depletion. The change in intracellular Ca^{2+} from Ca^{2+}-free solution to 2 mmol/L Ca^{2+} solution ($\Delta F_{340}/F_{380}$) was used to represent Ca^{2+} entry.

Statistical analysis

All quantitative data were expressed as the mean ± standard error of the mean. Paired *t*-test, Mann–Whitney rank-sum test, and one-way repeated measures ANOVA test with a post hoc Fisher's least significant difference test were used to compare atrial fibroblasts under different conditions. A *P* value of <0.05 was considered statistically significant.

Results

VEGF effects on the proliferation, migration, and collagen production of atrial fibroblasts

Compared with control cells, after treatment with VEGF for 48 h, atrial fibroblasts exhibited greater migratory capability,

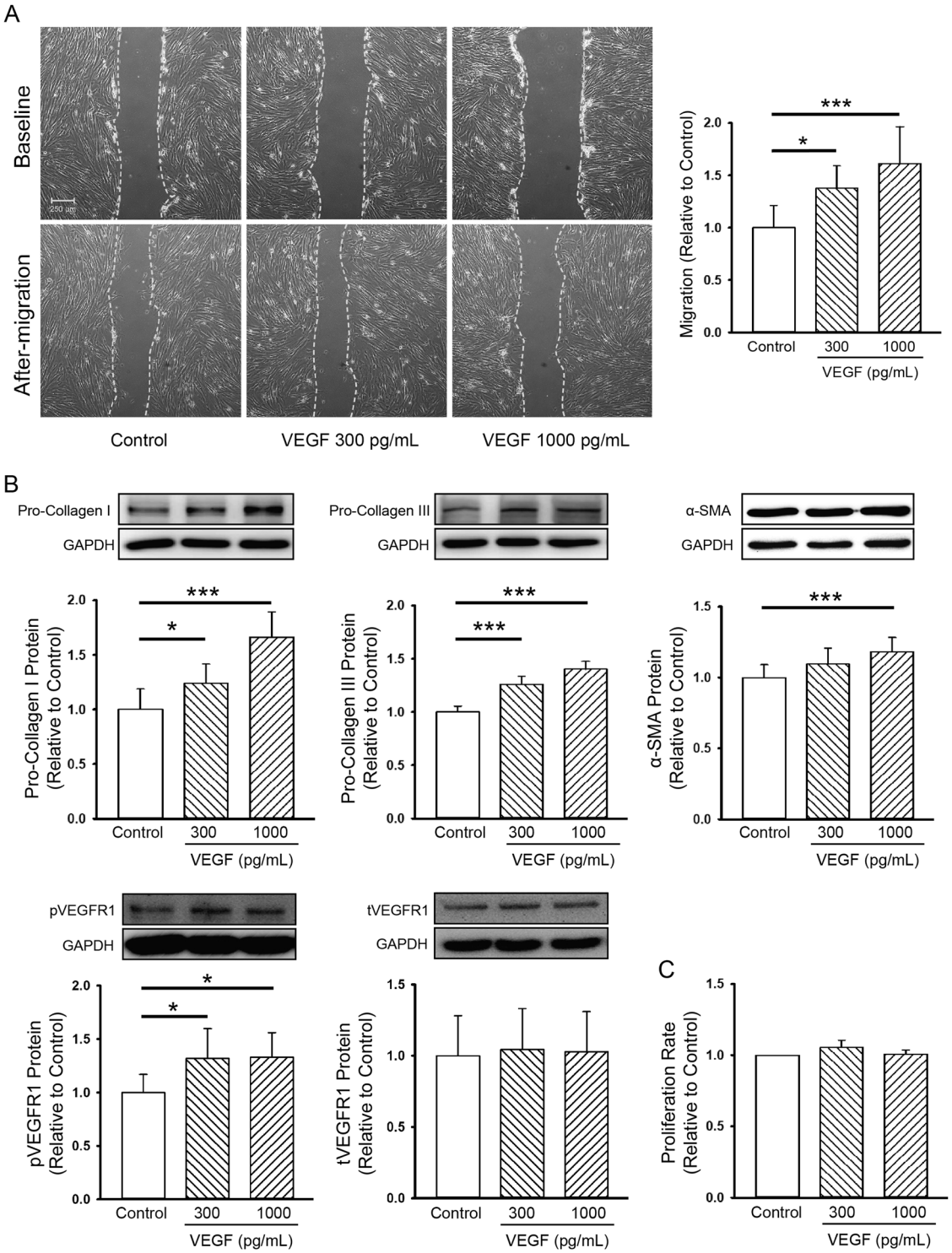

Fig. 1 Cell migration, collagen production, myofibroblast differentiation, signal transduction, and proliferation capabilities in atrial fibroblasts treated with vascular endothelial growth factor (VEGF). **a** Photographs and averaged data reveal the migration assay results of atrial fibroblasts treated with VEGF. Left upper panels show the initial scratch (baseline) in different groups. Left lower panels show the images 6 h after the scratch was created (after migration) ($n = 6$ independent experiments). **b** Photographs and averaged data reveal the pro-collagen type I production ($n = 7$ independent experiments), pro-collagen type III production ($n = 6$ independent experiments), α-smooth muscle actin (SMA, $n = 4$ independent experiments), phosphorylated VEGF receptor type I (pVEGFR1; $n = 7$ independent experiments), and total VEGFR1 (tVEGFR1; $n = 7$ independent experiments) in atrial fibroblasts treated with VEGF for 48 h. **c** VEGF treatment for 24 h had no significant effect on the proliferation rate of atrial fibroblasts ($n = 5$ independent experiments). GAPDH was used as a loading control. $^{*}p < 0.05$, $^{***}p < 0.005$

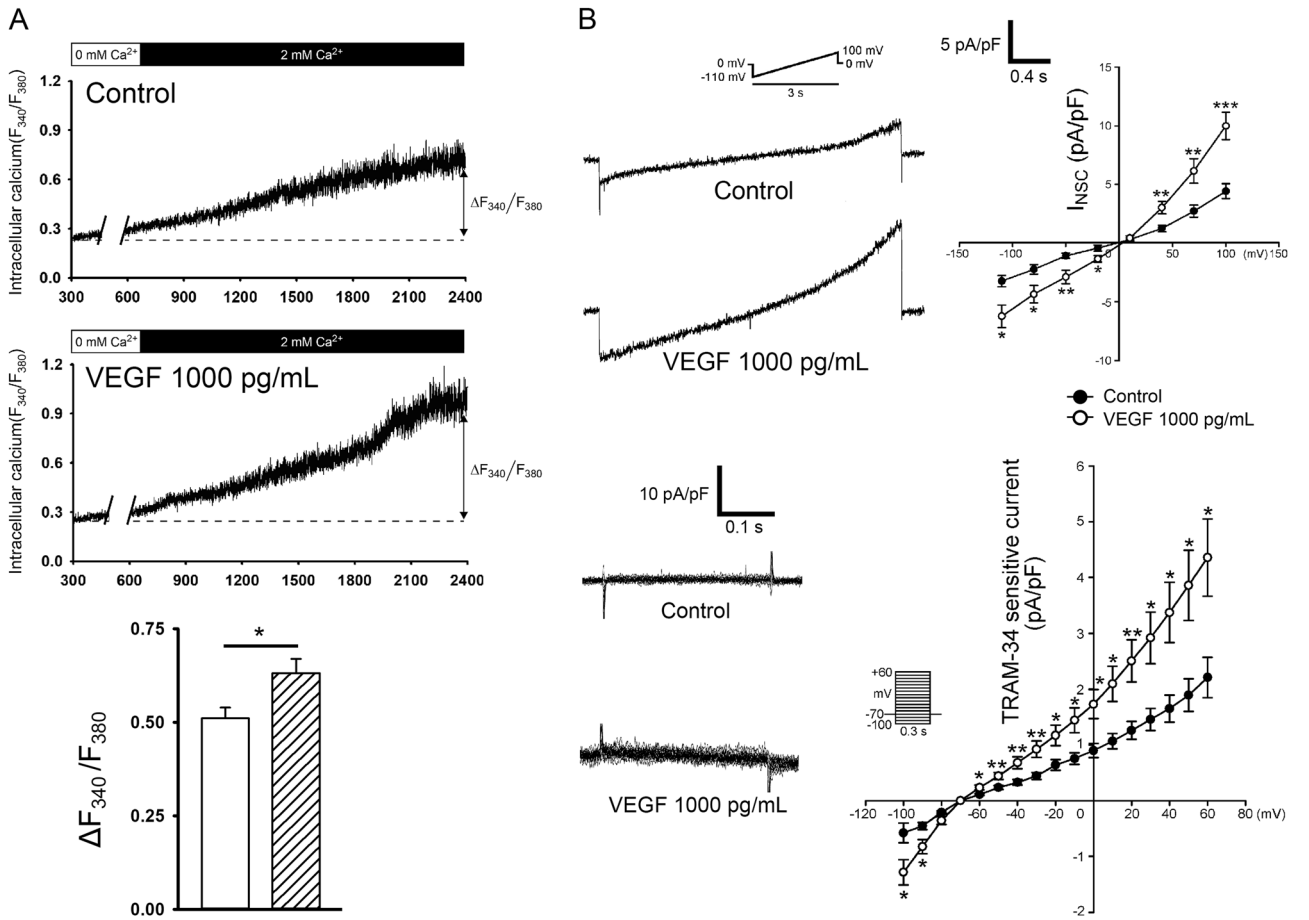

Fig. 2 Calcium entry, membrane currents of transient receptor potential (TRP) channels, and intermediate-conductance calcium-activated K^+ channels ($K_{Ca}3.1$) in vascular endothelial growth factor (VEGF)-treated atrial fibroblasts. **a** Upper panels reveal representative intracellular calcium (Ca^{2+}) tracing from control (upper tracing) and VEGF-treated (1000 pg/mL; lower tracing) atrial fibroblasts. Cells that had already been treated for 48 h, were first incubated with a Ca^{2+} free extracellular solution to deplete Ca^{2+} stores. Ca^{2+} entry was found after increasing extracellular Ca^{2+} to 2 mmol/L. lower panel shows the averaged change in intracellular Ca^{2+} from Ca^{2+} free solution to 2 mmol/L Ca^{2+} solution (change in the ratio of fluorescence due to excitation at 340 nm to that at 380 nm [$\Delta F_{340}/F_{380}$]). VEGF significantly increased Ca^{2+} influx in atrial fibroblasts ($n = 32$ cells from three independent experiments). **b** Upper panels reveal tracings and I/V relationship of the Gadolinium (100 μmol/L) sensitive nonselective cation current (I_{NSC}) from control ($n = 15$) and VEGF (1000 pg/mL)-treated ($n = 18$) atrial fibroblasts. Lower panels reveal tracings and I/V relationship of the TRAM-34 (1 μmol/L) sensitive potassium current from control ($n = 11$) and VEGF (1000 pg/mL)-treated ($n = 12$) atrial fibroblasts. $^*p < 0.05$, $^{**}p < 0.01$, $^{***}p < 0.005$. The insets in the current traces show the various clamp protocols

and higher expression of pVEGFR1, pro-collagen type I protein, pro-collagen type III protein, and α-SMA (a myofibroblast differentiation marker) protein expression (Fig. 1). However, control and VEGF-treated atrial fibroblasts had similar tVEGFR1 protein expression, and proliferation rate (Fig. 1).

Ca^{2+} entry and downstream signaling in VEGF-treated atrial fibroblasts

As shown in Fig. 2a, VEGF-treated (1000 pg/mL) atrial fibroblasts exhibited a greater Ca^{2+} entry. VEGF-treated (1000 pg/mL) atrial fibroblasts had upregulated currents through TRP and $K_{Ca}3.1$ channels (Fig. 2b). The enhanced Ca^{2+} entry in VEGF-treated (1000 pg/mL) atrial fibroblasts was attenuated with the TRP channel inhibitor (gadolinium, 100 μmol/L) or $K_{Ca}3.1$ inhibitor (TRAM-34, 1 μmol/L, Fig. 3a). Atrial fibroblasts treated with a combination of VEGF (1000 pg/mL) and the KCa3.1 inhibitor (TRAM-34, 1 μmol/L) exhibited lower I_{NSC}, than those treated with VEGF alone (Fig. 3b). As shown in Fig. 4a, VEGF-treated (1000 pg/mL for 5 min) atrial fibroblasts had a greater phosphorylated ERK than control atrial fibroblasts. However, control and VEGF-treated (1000 pg/mL for 5 min) atrial fibroblasts had similar phosphorylated p38 expression. Atrial fibroblasts treated with the combination of VEGF and the ERK inhibitor (PD98059, 50 μmol/L) had lower I_{NSC} than those treated with VEGF alone (Fig. 4b). The enhanced migratory, pro-collagen type I, pro-collagen type III, and α-SMA expression capabilities of VEGF-treated atrial

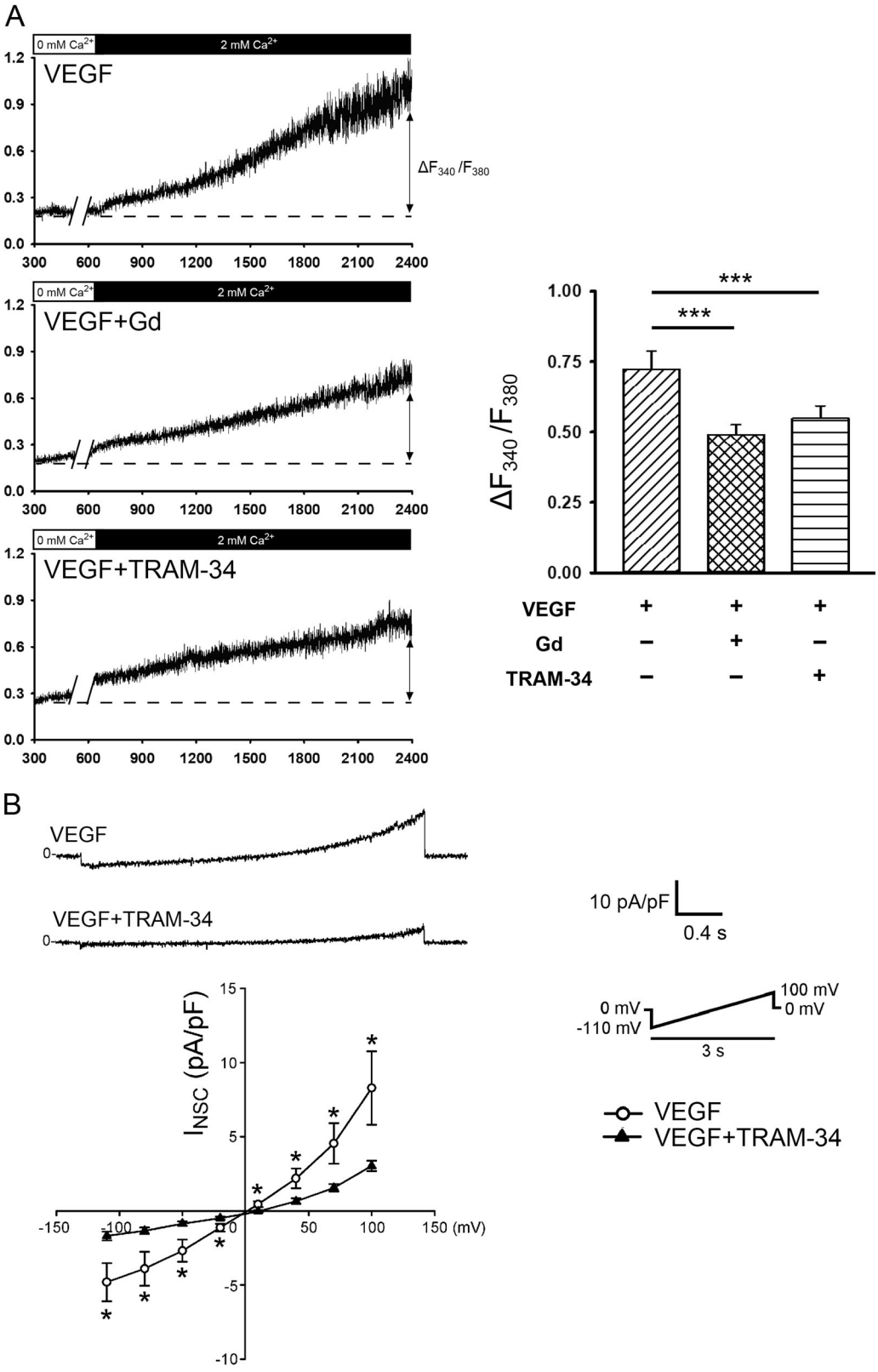

fibroblasts were attenuated by EGTA at 1 mmol/L (Figs. 5 and 6). VEGF-treated atrial fibroblasts had a larger phosphorylated CaMKII than control atrial fibroblasts (Fig. 6). However, control and VEGF-treated atrial fibroblasts had similar total CaMKII (Fig. 6). The upregulated phosphorylated CaMKII of VEGF-treated atrial fibroblasts could

Fig. 3 Interaction between transient receptor potential (TRP) channels, intermediate-conductance calcium (Ca^{2+})-activated K^+ channels ($K_{Ca}3.1$) and Ca^{2+} entry in vascular endothelial growth factor (VEGF)-treated atrial fibroblasts. **a** Representative Ca^{2+} influx tracing and average change in intracellular Ca^{2+} from Ca^{2+} free solution to 2 mmol/L Ca^{2+} solution (change in ratio of fluorescence due to excitation at 340 nm to that at 380 nm [$\Delta F_{340}/F_{380}$]) from atrial fibroblasts treated with VEGF (1000 pg/mL, $n = 22$), VEGF plus Gadolinium (Gd, 100 μmol/L, $n = 24$), or VEGF plus TRAM-34 (1 μmol/L, $n = 24$). **b** Tracings and I/V relationship reveal the gadolinium-sensitive (100 μmol/L) nonselective cation current (I_{NSC}) from atrial fibroblasts treated with VEGF (1000 pg/mL, $n = 14$), and those treated with VEGF plus TRAM-34 (1 μmol/L, $n = 14$). The insets in the current traces show the various clamp protocols. $^*p < 0.05$, $^{***}p < 0.005$

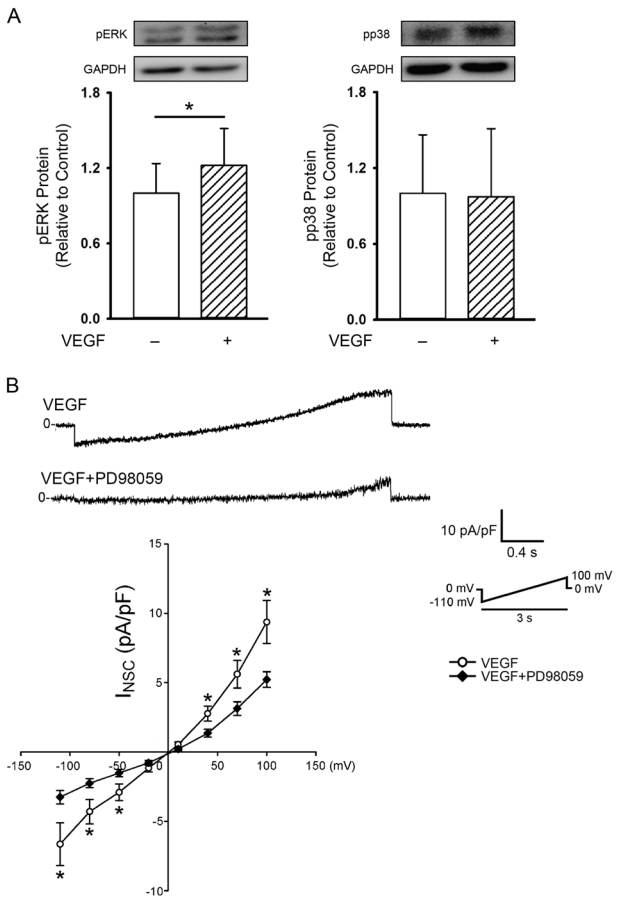

Fig. 4 Downstream signaling of vascular endothelial growth factor (VEGF)-treated atrial fibroblasts. **a** Photographs and averaged data show the phosphorylated ERK (pERK, $n = 6$ independent experiments), and phosphorylated p38 (pp38, $n = 6$ independent experiments) in atrial fibroblasts treated with VEGF (1000 pg/mL) for 5 min. GAPDH was used as a loading control. **b** Tracings and I/V relationship reveal the gadolinium-sensitive (100 μmol/L) nonselective cation current (I_{NSC}) from atrial fibroblasts treated with VEGF (1000 pg/mL, $n = 11$), and those treated with VEGF plus ERK inhibitor (PD98059 50 μmol/L, $n = 12$). The insets in the current traces show the various clamp protocols. $^*p < 0.05$

also be attenuated with EGTA at 1 mmol/L (Fig. 6). Moreover, the increased migratory capability and the expressions of pro-collagen type I, pro-collagen type III, and α-SMA in VEGF-treated atrial fibroblasts were blocked by KN93 (Fig. 7).

Discussion

VEGF is associated with endothelial dysfunction and tissue hypoxia in cardiovascular diseases. Our previous study has shown that VEGF enhanced collagen production capability of left atrial fibroblasts [14], but the mechanisms were not fully elucidated. To our knowledge, in this study in human atrial fibroblasts, for the first time, we found that VEGF (1000 pg/mL) enhanced collagen production, and migration, and myofibroblast differentiation in atrial fibroblasts. Moreover, VEGF significantly increased Ca^{2+} entry, which is recognized as the fundamental signaling pathway in fibrogenesis. In addition, lower extracellular Ca^{2+} by EGTA blocked the profibrotic effects of VEGF on the fibroblasts migratory capability, collagen production ability, and myofibroblast differentiation capability, which suggests that augmented Ca^{2+} influx may contribute to the profibrotic effects of VEGF. The Ca^{2+} signaling pathway critically regulates the activities of multiple profibrotic growth factors. Activation of ryanodine channel-induced Ca^{2+} entry by the transforming growth factor was shown to increase collagen type I gene expression in fibroblasts [15]. The increase in intracellular Ca^{2+} by evoking inositol trisphosphate signaling may induce the genesis of collagen type I in fibroblasts [16]. Our findings provide benchside evidence leading to a potential novel strategy targeting atrial myopathy and arrhythmofibrosis. The concentration of VEGF in the present study was similar to the known higher plasma concentration in patients with AF (120–1400 pg/mL) [24]. Accordingly, the biological effects of VEGF in human atrial fibroblasts are expected to be clinically relevant.

TRP channels, which are Ca^{2+} entry channels activated by various pathological stimuli and cell stretch [25], are highly associated with cardiac fibrosis in a plethora of studies. TRP channels are upregulated in patients with atrial fibrosis [26]. Overexpressing TRP channels exhibited higher myocardial fibrosis in mice [27]. Blocking TRP channels suppresses angiotensin II-induced Ca^{2+} influx, collagen production, and myofibroblast differentiation in atrial fibroblasts [28]. Activated $K_{Ca}3.1$ channels induce membrane hyperpolarization and consequently trigger more persistent Ca^{2+} entry through TRP channels or other voltage-gated channels [29]. Blockade of $K_{Ca}3.1$ by TRAM-34 decreases Ca^{2+} entry [30], attenuates myocardial fibrosis in post-myocardial infarction rats [31] and decreases collagen production and myofibroblast differentiation capability of renal fibroblasts [32]. In line with previous studies, we found that VEGF significantly increased the currents of TRP and $K_{Ca}3.1$ channels, which contribute to the high Ca^{2+} entry in

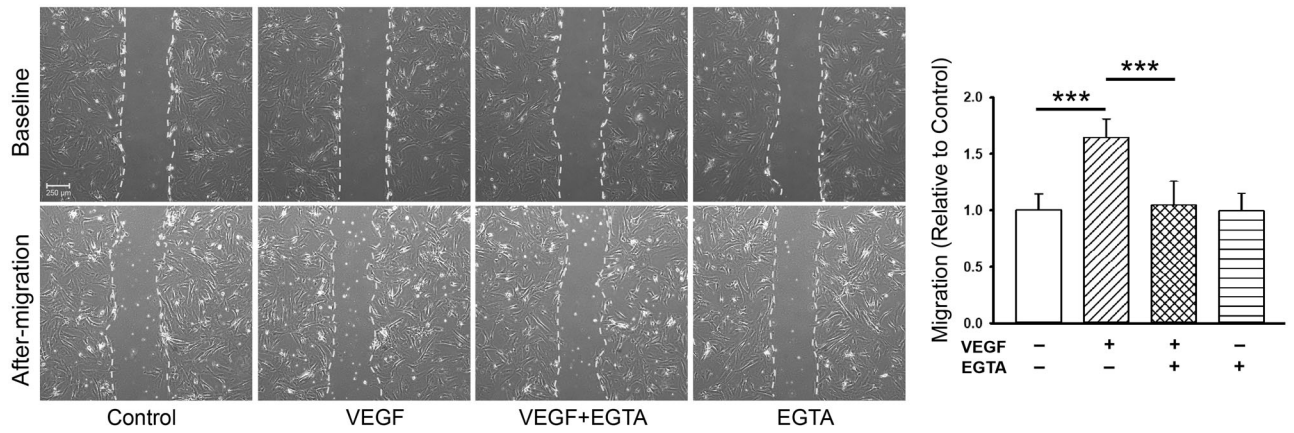

Fig. 5 The effects of ethylene glycol tetra-acetic acid (EGTA) on vascular endothelial growth factor (VEGF) increased migration in atrial fibroblasts. Photographs and averaged data show the migration assay in VEGF-treated (1000 pg/ mL) atrial fibroblasts with or without EGTA (1 mmol/L). Upper panels show the initial scratch (baseline) in different groups. Lower panels show the images 6 h after the scratch was created (after migration) ($n = 8$ independent experiments). $^{***}p < 0.005$

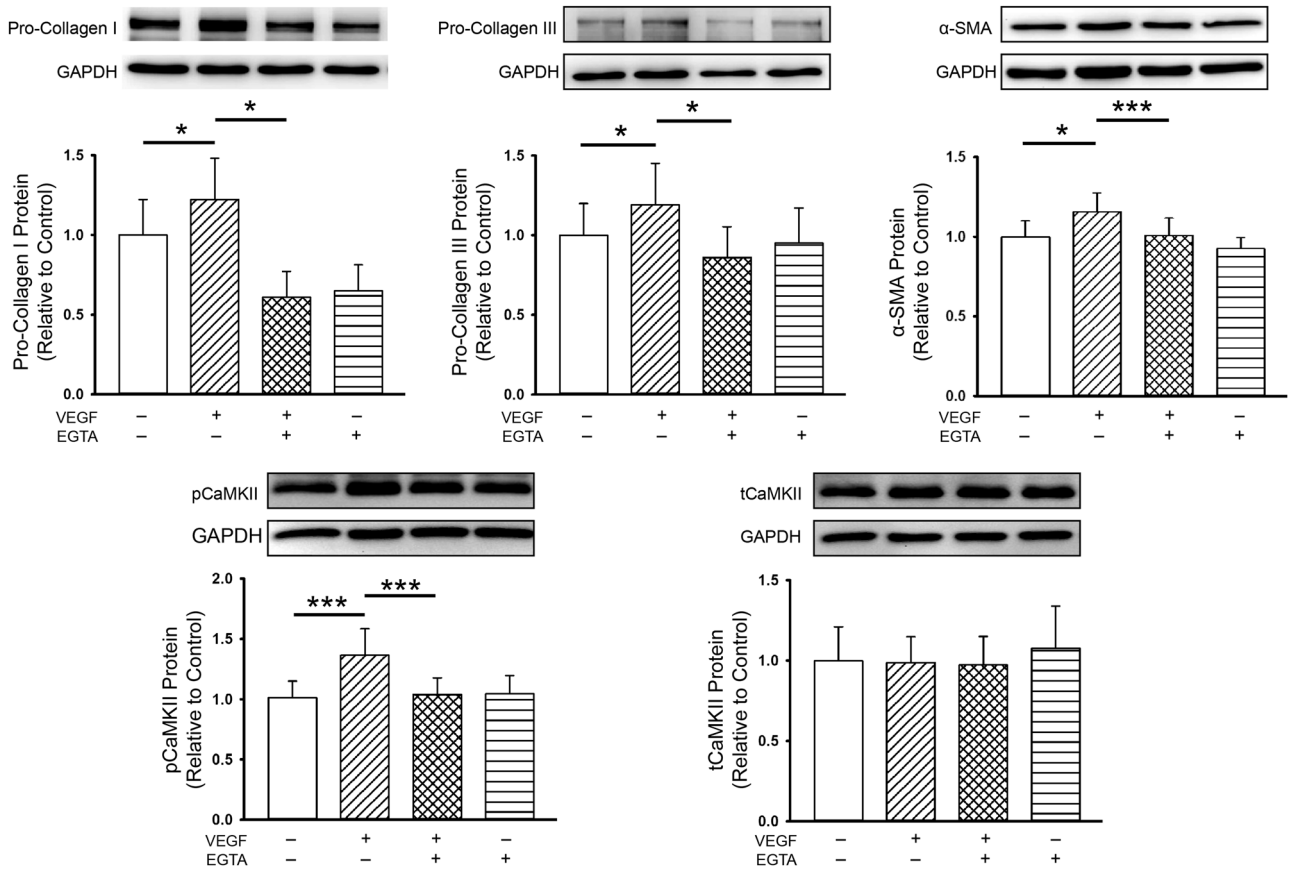

Fig. 6 The effects of ethylene glycol tetra-acetic acid (EGTA) on vascular endothelial growth factor (VEGF) increased profibrotic signaling in atrial fibroblasts. Photographs and averaged data show the pro-collagen type I production ($n = 5$ independent experiments), pro-collagen type III production ($n = 7$ independent experiments), α-smooth muscle actin (SMA, $n = 7$ independent experiments), phosphorylated Ca^{2+}/calmodulin-dependent protein kinase II (pCaMKII, $n = 6$ independent experiments), and total CaMKII (tCaMKII, $n = 6$ independent experiments) in VEGF-treated (1000 pg/mL) atrial fibroblasts with or without EGTA (1 mmol/L) for 48 h. GAPDH was used as a loading control. $^{*}p < 0.05$, $^{***}p < 0.005$

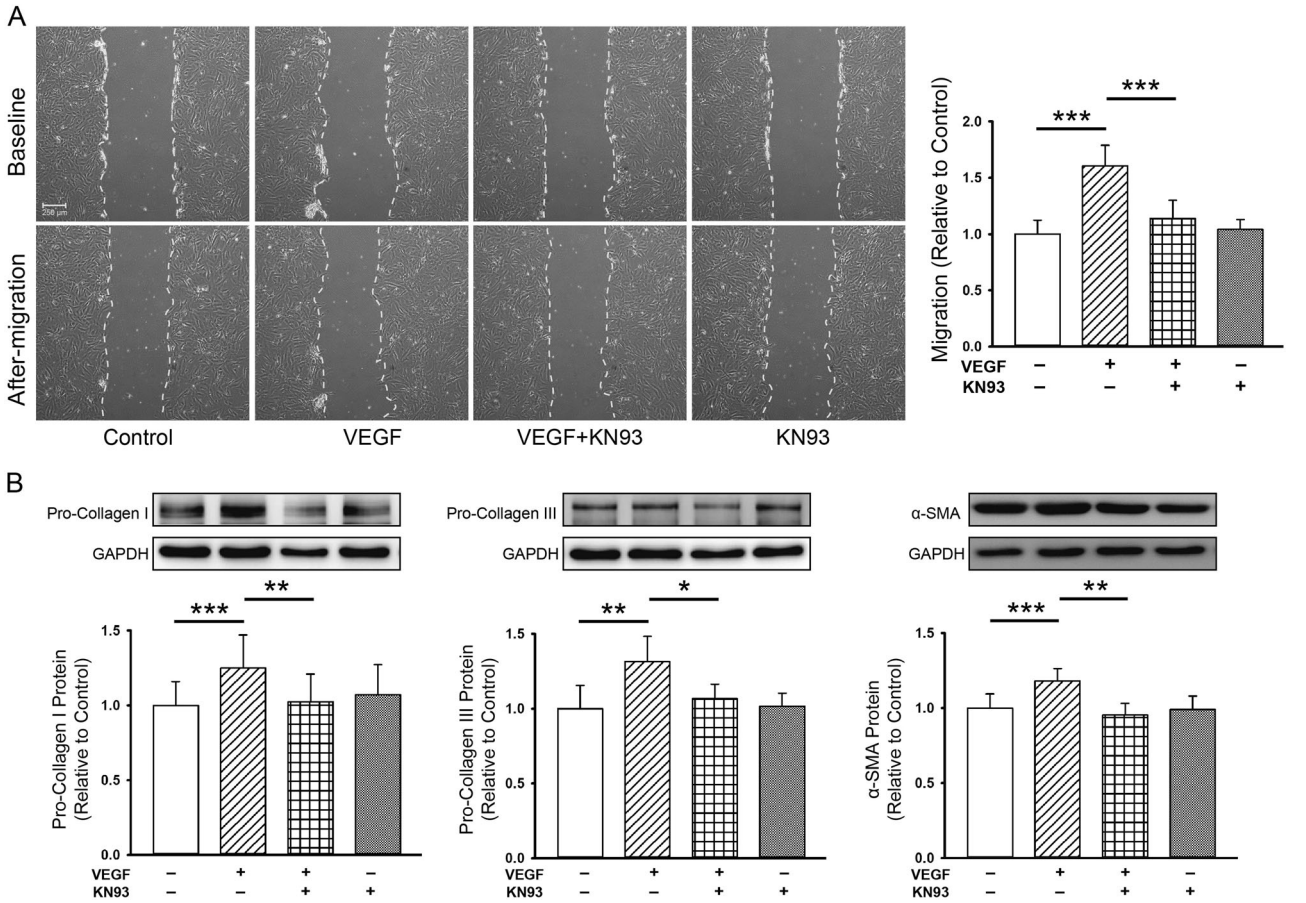

Fig. 7 The effects of KN93, the Ca^{2+}/calmodulin-dependent protein kinase II (CaMKII) inhibitor, on vascular endothelial growth factor (VEGF)-treated atrial fibroblasts. **a** Photographs and averaged data show the migration assay in VEGF-treated (1000 pg/mL) atrial fibroblasts with or without KN93 (10 μmol/L). Upper panels show the initial scratch (baseline) in different groups. Lower panels show the images 6 h after the scratch was created (after migration) ($n = 6$ independent experiments). **b** Photographs and averaged data show the pro-collagen type I production ($n = 6$ independent experiments), pro-collagen type III production ($n = 5$ independent experiments), and α-smooth muscle actin (SMA, $n = 6$ independent experiments) in VEGF (1000 pg/mL)-treated atrial fibroblasts with or without KN93 (10 μmol/L) for 48 h. GAPDH was used as a loading control. $^{*}p < 0.05$, $^{**}p < 0.01$, $^{***}p < 0.005$

Ca^{2+} imaging assays. In addition, this study found that TRAM-34 attenuated the effects of VEGF on I_{NSC} in atrial fibroblasts, further confirming the interaction of TRP channels and $K_{Ca}3.1$ channels upon Ca^{2+} entry.

VEGF-A induces VEGFR1 auto-phosphorylation thereby transmitting various downstream signaling [33–35]. Autophosphorylated VEGFR1 activate profibrotic ERK [36] and p38 [37] signaling pathways [38]. In this study, VEGF was found to upregulate the expressions of phosphorylated VEGFR1 and phosphorylated ERK, but not p38, in atrial fibroblasts. Inhibition of the ERK signaling pathway decreased I_{NSC} through TRP channels in VEGF-treated atrial fibroblasts, which may indicate that VEGF activates TRP channels through ERK signaling. Similarly, a previous study showed that ERK inhibition attenuated TRP channel-dependent Ca^{2+} entry [39] and that TRP channels mediated inward currents can be activated through the ERK signaling pathway [40].

CaMKII is the downstream messenger of Ca^{2+} signaling. Binding of Ca^{2+}/calmodulin triggers CaMKII auto-phosphorylation [41], thereby activating the profibrotic signaling, such as ERK [42], or NF-κB [43] signaling pathway. Pharmacological blockade of CaMKII by KN93 or genetically knocking down CaMKII decreases cardiac fibrosis in pathological left ventricular remodeling [44, 45]. In addition, the activation of CaMKII promotes collagen production and the migratory capability of fibroblasts [46, 47]. In this study, we found that VEGF upregulated phosphorylated CaMKII, but not total CaMKII, suggesting that VEGF modulates Ca^{2+} homeostasis in atrial fibroblasts through phosphorylated CaMKII, but not non-phosphorylated CaMKII. In addition, the profibrotic cellular activities and upregulated phosphorylated CaMKII of VEGF-treated atrial fibroblasts could be decreased with EGTA. Moreover, inhibiting CaMKII activity by KN93 decreased the VEGF-augmented migration, collagen

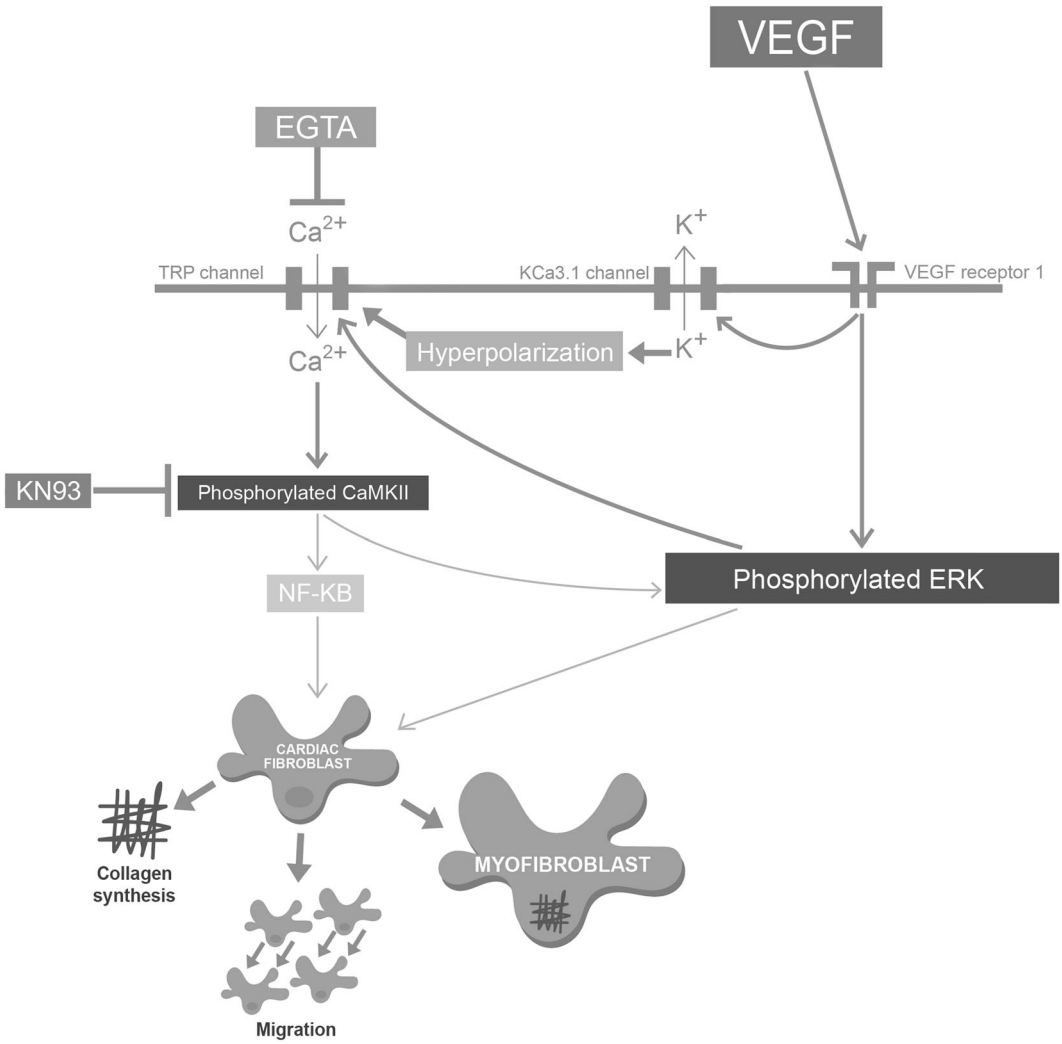

Fig. 8 Illustration showing the proposed molecular mechanism of the profibrotic effects of vascular endothelial growth factor (VEGF) on atrial fibroblasts. VEGF increases Ca^{2+} entry via the ERK signaling and the interaction of transient receptor potential (TRP) and intermediate-conductance calcium-activated K^+ ($K_{Ca}3.1$) channels thereby activating the collagen production, migratory capability and myofibroblast differentiation of atrial fibroblasts through the Ca^{2+}/calmodulin-dependent protein kinase II (CaMKII)/ERK, NF-κB signal pathway. EGTA ethylene glycol tetra-acetic acid, KN93 CaMKII inhibitor

production, and myofibroblast differentiation capabilities of atrial fibroblasts. These findings suggest that VEGF upregulated CaMKII signaling through Ca^{2+} influx and consequently triggered the profibrotic activities of atrial fibroblasts.

In conclusion, as summarized in Fig. 8, VEGF increases atrial fibroblast activity through CaMKII signaling by enhancing Ca^{2+} entry.

Acknowledgements The authors acknowledge the technical services of calcium image experiments provided by Instrument Center of National Defense Medical Center.

Funding This work was supported by the Taipei Medical University—Wan Fang Hospital [107TMU-WFH-01-3] and the Ministry of Science and Technology of Taiwan (MOST 106-2314-B-038-055).

Compliance with ethical standards

Conflict of interest The authors declare that they have no conflict of interest.

Publisher's note Springer Nature remains neutral with regard to jurisdictional claims in published maps and institutional affiliations.

References

1. Ogi H, Nakano Y, Niida S, Dote K, Hirai Y, Suenari K, et al. Is structural remodeling of fibrillated atria the consequence of tissue hypoxia? Circ J. 2010;74:1815–21.
2. Matsudaira K, Maeda K, Okumura N, Yoshikawa D, Morita Y, Mitsuhashi H, et al. Impact of low levels of vascular endothelial growth factor after myocardial infarction on 6-month clinical

outcome. Results from the Nagoya Acute Myocardial Infarction Study. Circ J. 2012;76:1509–16.
3. Van Craenenbroeck EM, Beckers PJ, Possemiers NM, Wuyts K, Frederix G, Hoymans VY, et al. Exercise acutely reverses dysfunction of circulating angiogenic cells in chronic heart failure. Eur Heart J. 2010;31:1924–34.
4. Scridon A, Morel E, Nonin-Babary E, Girerd N, Fernandez C, Chevalier P. Increased intracardiac vascular endothelial growth factor levels in patients with paroxysmal, but not persistent atrial fibrillation. Europace. 2012;14:948–53.
5. Gramley F, Lorenzen J, Jedamzik B, Gatter K, Koellensperger E, Munzel T, et al. Atrial fibrillation is associated with cardiac hypoxia. Cardiovasc Pathol. 2010;19:102–11.
6. Abe I, Teshima Y, Kondo H, Kaku H, Kira S, Ikebe Y, et al. Association of fibrotic remodeling and cytokines/chemokines content in epicardial adipose tissue with atrial myocardial fibrosis in patients with atrial fibrillation. Heart Rhythm. 2018;15:1717–27.
7. Berntsson J, Smith JG, Johnson LSB, Söderholm M, Borné Y, Melander O, et al. Increased vascular endothelial growth factor D is associated with atrial fibrillation and ischaemic stroke. Heart. 2019;105:553–8.
8. Iwasaki YK, Yamashita T, Sekiguchi A, Hayami N, Shimizu W. Importance of pulmonary vein preferential fibrosis for atrial fibrillation promotion in hypertensive rat hearts. Can J Cardiol. 2016;32:767–76.
9. Lottonen-Raikaslehto L, Rissanen R, Gurzeler E, Merentie M, Huusko J, Schneider JE, et al. Left ventricular remodeling leads to heart failure in mice with cardiac-specific overexpression of VEGF-B167: echocardiography and magnetic resonance imaging study. Physiol Rep. 2017;5:e13096.
10. Bondarenko NA, Nikonorova YV, Surovtseva MA, Lykov AP, Poveshchenko OV, Poveshchenko AF, et al. Effect of vascular endothelial growth factor and erythropoietin on functional activity of fibroblasts and multipotent mesenchymal stromal cells. Bull Exp Biol Med. 2016;160:498–501.
11. Zhao T, Zhao W, Meng W, Liu C, Chen Y, Bhattacharya SK, et al. Vascular endothelial growth factor-D mediates fibrogenic response in myofibroblasts. Mol Cell Biochem. 2016;413:127–35.
12. Park HY, Kim JH, Park CK. VEGF induces TGF-β1 expression and myofibroblast transformation after glaucoma surgery. Am J Pathol. 2013;182:2147–54.
13. Cao X, Xia H, Li N, Xiong K, Wang Z, Wu S. A mechanical refractory period of chondrocytes after dynamic hydrostatic pressure. Connect Tissue Res. 2015;56:212–8.
14. Chung CC, Kao YH, Yao CJ, Lin YK, Chen YJ. A comparison of left and right atrial fibroblasts reveals different collagen production activity and stress-induced mitogen-activated protein kinase signalling in rats. Acta Physiol. 2017;220:432–45.
15. Mukherjee S, Kolb MR, Duan F, Janssen LJ. Transforming growth factor-β evokes Ca^{2+} waves and enhances gene expression in human pulmonary fibroblasts. Am J Respir Cell Mol Biol. 2012;46:757–64.
16. Mukherjee S, Duan F, Kolb MR, Janssen LJ. Platelet derived growth factor-evoked Ca^{2+} wave and matrix gene expression through phospholipase C in human pulmonary fibroblast. Int J Biochem Cell Biol. 2013;45:1516–24.
17. Zhang B, Jiang J, Yue Z, Liu S, Ma Y, Yu N, et al. Store-Operated Ca^{2+} Entry (SOCE) contributes to angiotensin II-induced cardiac fibrosis in cardiac fibroblasts. J Pharmacol Sci. 2016;132:171–80.
18. Ikeda K, Nakajima T, Yamamoto Y, Takano N, Tanaka T, Kikuchi H, et al. Roles of transient receptor potential canonical (TRPC) channels and reverse-mode Na^+/Ca^{2+} exchanger on cell proliferation in human cardiac fibroblasts: effects of transforming growth factor β1. Cell calcium. 2013;54:213–25.
19. Murata N, Ito S, Furuya K, Takahara N, Naruse K, Aso H, et al. Ca^{2+} influx and ATP release mediated by mechanical stretch in human lung fibroblasts. Biochem Biophys Res Commun. 2014;453:101–5.
20. Yang S, Huang XY. Ca^{2+} influx through L-type Ca^{2+} channels controls the trailing tail contraction in growth factor-induced fibroblast cell migration. J Biol Chem. 2005;280:27130–7.
21. Wellner M, Maasch C, Kupprion C, Lindschau C, Luft FC, Haller H. The proliferative effect of vascular endothelial growth factor requires protein kinase C-α and protein kinase C-ζ. Arterioscler Thromb Vasc Biol. 1999;19:178–85.
22. Chung CC, Hsu RC, Kao YH, Liou JP, Lu YY, Chen YJ. Androgen attenuates cardiac fibroblasts activations through modulations of transforming growth factor-β and angiotensin II signaling. Int J Cardiol. 2014;176:386–93.
23. Qi XY, Huang H, Ordog B, Luo X, Naud P, Sun Y, et al. Fibroblast inward-rectifier potassium current upregulation in profibrillatory atrial remodeling. Circ Res. 2015;116:836–45.
24. Chung NA, Belgore F, Li-Saw-Hee FL, Conway DS, Blann AD, Lip GY. Is the hypercoagulable state in atrial fibrillation mediated by vascular endothelial growth factor? Stroke. 2002;33:2187–91.
25. Yue L, Xie J, Nattel S. Molecular determinants of cardiac fibroblast electrical function and therapeutic implications for atrial fibrillation. Cardiovasc Res. 2011;89:744–53.
26. Zhang YJ, Ma N, Su F, Liu H, Mei J. Increased TRPM6 expression in atrial fibrillation patients contribute to atrial fibrosis. Exp Mol Pathol. 2015;98:486–90.
27. Kuwahara K, Wang Y, McAnally J, Richardson JA, Bassel-Duby R, Hill JA, et al. TRPC6 fulfills a calcineurin signaling circuit during pathologic cardiac remodeling. J Clin Investig. 2006;116:3114–26.
28. Harada M, Luo X, Qi XY, Tadevosyan A, Maguy A, Ordog B, et al. Transient receptor potential canonical-3 channel-dependent fibroblast regulation in atrial fibrillation. Circulation. 2012;126:2051–64.
29. Chandy KG, Wulff H, Beeton C, Pennington M, Gutman GA, Cahalan MD. K^+ channels as targets for specific immunomodulation. Trends Pharmacol Sci. 2004;25:280–9.
30. Steudel FA, Mohr CJ, Stegen B, Nguyen HY, Barnert A, Steinle M, et al. SK4 channels modulate Ca^{2+} signalling and cell cycle progression in murine breast cancer. Mol Oncol. 2017;11:1172–88.
31. Ju CH, Wang XP, Gao CY, Zhang SX, Ma XH, Liu C. Blockade of $K_{Ca}3.1$ attenuates left ventricular remodeling after experimental myocardial infarction. Cell Physiol Biochem. 2015;36:1305–15.
32. Huang C, Shen S, Ma Q, Gill A, Pollock CA, Chen XM. $K_{Ca}3.1$ mediates activation of fibroblasts in diabetic renal interstitial fibrosis. Nephrol Dial Transplant. 2014;29:313–24.
33. Takahashi H, Shibuya M. The vascular endothelial growth factor (VEGF)/VEGF receptor system and its role under physiological and pathological conditions. Clin Sci. 2005;109:227–41.
34. Shibuya M, Claesson-Welsh L. Signal transduction by VEGF receptors in regulation of angiogenesis and lymphangiogenesis. Exp Cell Res. 2006;312:549–60.
35. Ito N, Huang K, Claesson-Welsh L. Signal transduction by VEGF receptor-1 wild type and mutant proteins. Cell Signal. 2001;13:849–54.
36. Sun C, Zhu M, Yang Z, Pan X, Zhang Y, Wang Q, et al. LL-37 secreted by epithelium promotes fibroblast collagen production: a potential mechanism of small airway remodeling in chronic obstructive pulmonary disease. Lab Investig. 2014;94:991–1002.
37. Luo YH, Ouyang PB, Tian J, Guo XJ, Duan XC. Rosiglitazone inhibits TGF-β 1 induced activation of human Tenon fibroblasts via p38 signal pathway. PLoS ONE. 2014;9:e105796.

38. Koch S, Tugues S, Li X, Gualandi L, Claesson-Welsh L. Signal transduction by vascular endothelial growth factor receptors. Biochem J. 2011;437:168–83.
39. Gomart S, Gaudreau-Ménard C, Jespers P, Dilek OG, Hupkens E, Hanthazi A, et al. Leptin-induced endothelium-independent vasoconstriction in thoracic aorta and pulmonary artery of spontaneously hypertensive rats: role of calcium channels and stores. PLoS ONE. 2017;12:e0169205–e0169205.
40. Kubota H, Nagao S, Obata K, Hirono M. mGluR1-mediated excitation of cerebellar GABAergic interneurons requires both G protein-dependent and Src-ERK1/2-dependent signaling pathways. PLoS ONE. 2014;9:e106316–e106316.
41. Means AR. Regulatory cascades involving calmodulin-dependent protein kinases. Mol Endocrinol. 2000;14:4–13.
42. Monaco S, Illario M, Rusciano MR, Gragnaniello G, Di Spigna G, Leggiero E, et al. Insulin stimulates fibroblast proliferation through calcium-calmodulin-dependent kinase II. Cell Cycle. 2009;8:2024–30.
43. Kim JE, Kim SY, Lim SY, Kieff E, Song YJ. Role of Ca^{2+}/calmodulin-dependent kinase II-IRAK1 interaction in LMP1-induced NF-κB activation. Mol Cell Biol. 2014;34:325–34.
44. Zhong P, Quan D, Peng J, Xiong X, Liu Y, Kong B, et al. Role of CaMKII in free fatty acid/hyperlipidemia-induced cardiac remodeling both in vitro and in vivo. J Mol Cell Cardiol. 2017;109:1–16.
45. Kreusser MM, Lehmann LH, Wolf N, Keranov S, Jungmann A, Gröne HJ, et al. Inducible cardiomyocyte-specific deletion of CaM kinase II protects from pressure overload-induced heart failure. Basic Res Cardiol. 2016;111:65.
46. Zhang W, Chen DQ, Qi F, Wang J, Xiao WY, Zhu WZ. Inhibition of calcium-calmodulin-dependent kinase II suppresses cardiac fibroblast proliferation and extracellular matrix secretion. J Cardiovasc Pharmacol. 2010;55:96–105.
47. House SJ, Singer HA. CaMKII-δ isoform regulation of neointima formation after vascular injury. Arterioscler Thromb Vasc Biol. 2008;28:441.